Journal of Biomechanics 46 (2013) 637–644

Contents lists available at SciVerse ScienceDirect

Journal of Biomechanics

journal homepage: www.elsevier.com/locate/jbiomech
www.JBiomech.com

2012 ASB Journal of Biomechanics Award

Altering prosthetic foot stiffness influences foot and muscle function during below-knee amputee walking: A modeling and simulation analysis

Nicholas P. Fey [a], Glenn K. Klute [b], Richard R. Neptune [a,*]

[a] Department of Mechanical Engineering, The University of Texas at Austin, 1 University Station C2200, TX 78712, USA
[b] Department of Veterans Affairs, Puget Sound Health Care System, Seattle, WA 98108, USA

ARTICLE INFO

Article history:
Accepted 30 November 2012

Keywords:
Gait
Biomechanics
Forward dynamics simulation
Elastic energy storage and return
Transtibial amputee

ABSTRACT

Most prosthetic feet are designed to improve amputee gait by storing and releasing elastic energy during stance. However, how prosthetic foot stiffness influences muscle and foot function is unclear. Identifying these relationships would provide quantitative rationale for prosthetic foot prescription that may lead to improved amputee gait. The purpose of this study was to identify the influence of altered prosthetic foot stiffness on muscle and foot function using forward dynamics simulations of amputee walking. Three 2D muscle-actuated forward dynamics simulations of unilateral below-knee amputee walking with a range of foot stiffness levels were generated, and muscle and prosthetic foot contributions to body support and propulsion and residual leg swing were quantified. As stiffness *decreased*, the prosthetic keel provided increased support and braking (negative propulsion) during the first half of stance while the heel contribution to support decreased. During the second half of stance, the keel provided decreased propulsion and increased support. In addition, the keel absorbed less power from the leg, contributing more to swing initiation. Thus, several muscle compensations were necessary. During the first half of stance, the residual leg hamstrings provided decreased support and increased propulsion. During the second half of stance, the *intact leg* vasti provided increased support and the residual leg rectus femoris transferred increased energy from the leg to the trunk for propulsion. These results highlight the influence prosthetic foot stiffness has on muscle and foot function throughout the gait cycle and may aid in prescribing feet of appropriate stiffness.

1. Introduction

Below-knee amputees commonly develop asymmetrical gait patterns and comorbidities in their residual and intact legs (Burke et al., 1978; Sanderson and Martin, 1997; Winter and Sienko, 1988). Prosthetic feet have been developed to minimize these asymmetries by utilizing elastic energy storage and return (ESAR) to help provide important walking subtasks including body support, forward propulsion and leg swing initiation, which are normally provided by the ankle plantar flexors in non-amputee walking (e.g., McGowan et al., 2009; Neptune et al., 2001). However, the influence of ESAR prosthetic foot stiffness on walking mechanics is not well-understood. One challenge to acquiring needed biomechanical data to identify this influence is the complexity of manufacturing custom feet with specific stiffness levels.

To overcome this challenge, we recently developed a manufacturing framework integrating selective laser sintering (SLS) to systematically vary a prosthetic foot design to assess the influence of foot stiffness on amputee kinematics, kinetics and muscle activity during walking (South et al., 2010; Fey et al., 2011). We found that decreasing foot stiffness increases the prosthesis range of motion, mid-stance energy storage and late-stance energy return that results in reduced residual leg hamstring activity. Thus, decreasing stiffness may enable ESAR prosthetic feet to provide additional forward propulsion and reduce the compensatory action of the hamstring muscles (Neptune et al., 2004). However, as stiffness decreased, a reduced residual leg vertical ground reaction force (GRF) and increased muscle activity of the residual leg vastus and gluteus medius, and intact leg vastus and rectus femoris were observed. These changes appear to be necessary to provide needed body support (Anderson and Pandy, 2003; Liu et al., 2006; Neptune et al., 2004). Thus, reduced residual leg hamstring contributions to forward propulsion during late-stance may be offset by needed muscle compensations to provide body support. Identifying the causal relationships between

* Corresponding author. Tel.: +512 471 0848; fax: +512 471 8727.
E-mail address: rneptune@mail.utexas.edu (R.R. Neptune).

0021-9290/$ - see front matter © 2012 Elsevier Ltd. All rights reserved.
http://dx.doi.org/10.1016/j.jbiomech.2012.11.051

prosthetic foot stiffness and muscle and prosthetic foot function would provide quantitative rationale for prosthetic foot prescription that might be otherwise difficult to discern using experimental techniques.

The purpose of this study was to identify the influence of prosthetic foot stiffness on muscle and foot function by developing forward dynamics simulations of below-knee amputee walking with a range of foot stiffness levels. Previously, forward dynamics simulations have provided insight into muscle contributions to body support, forward propulsion and leg swing walking subtasks (e.g., Anderson and Pandy, 2003; Liu et al., 2006; McGowan et al., 2009; Neptune et al., 2004). Based on our previously-observed experimental findings, we tested the hypotheses that as stiffness decreases, foot contributions to forward propulsion and leg swing initiation would increase, and therefore muscle contributions to these subtasks would decrease. Also as stiffness decreases, we expected that foot contributions to body support would decrease, and therefore muscle contributions to body support would increase.

2. Methods

2.1. Bipedal musculoskeletal model

Forward dynamics simulations of unilateral below-knee amputee walking were generated using a planar bipedal musculoskeletal model (Fig. 1) developed using SIMM/Dynamics Pipeline (MusculoGraphics, Inc.). The model used was similar to previous analyses of walking (McGowan et al., 2009; Neptune et al., 2001) and consisted of rigid trunk, thigh and shank segments. Segments also represented the talus, calcaneus, mid-foot and toes of the intact leg foot. Musculoskeletal geometry was based on Delp et al. (1990). Residual leg shank inertial properties were based on Mattes et al. (2000). The trunk had two translational and one rotational degrees-of-freedom, while revolute joints modeled flexion/extension of the hip joints. The knees were modeled using planar joints, with a flexion/extension rotation and the two translational degrees-of-freedom prescribed as a function of knee flexion angle. Revolute joints modeled flexion/extension of the ankle, subtalar and metatarsophalangeal joints of the intact leg. Therefore, not including the prosthetic foot, the model had 10 degrees-of-freedom. Passive torques representing joint structures and tissues were applied (Anderson and Pandy, 1999; Davy and Audu, 1987), and 31 visco-elastic elements with coulomb friction were attached beneath each foot to model foot-ground contact (Neptune et al., 2000). The system equations of motion were generated using SD/FAST (PTC).

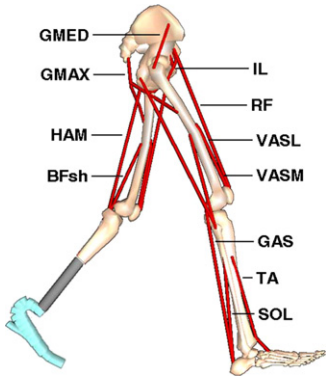

Fig. 1. The amputee musculoskeletal model was actuated by 25 Hill-type musculotendon actuators in the intact leg categorized into 14 muscle groups based on anatomical classification, with actuators in each group receiving the same excitation pattern. These muscle groups were: GMED (anterior and posterior compartments of the gluteus medius), GMAX (gluteus maximus, adductor magnus), HAM (biceps femoris long head, medial hamstrings), BFsh (biceps femoris short head), IL (psoas, iliacus), RF (rectus femoris), VASL (vastuslateralis, vastusintermedius), VASM (vastusmedialis), GAS (medial and lateral gastrocnemius), SOL (soleus, tibialis posterior), TA (tibialis anterior, peroneus tertius), PR (peroneus longus, peroneus brevis), FLXDG (flexor digitorumlongus, flexor hallucislongus) and EXTDG (extensor digitorumlongus, extensor hallucislongus). For figure clarity, the smaller muscle groups that control the foot (PR, FLXDG and EXTDG) are not shown. The residual leg had the same muscle groups except for the muscles that span the ankle (GAS, SOL, TA, PR, FLXDG and EXTDG) since these muscles are either removed or severely altered during a below-knee amputation.

2.2. Hill-type musculotendon actuators

Hill-type musculotendon actuators governed by intrinsic muscle force-length-velocity relationships (Zajac, 1989) were used to drive the model. Similar to previous work (Hall et al., 2011), excitation patterns were parameterized using a bimodal equation:

$$e(t)=\sum_{i=1}^{2}\begin{cases}\frac{a_i}{2}\left[1-\cos\left(\frac{2\pi(t-\text{onset}_i)}{\text{offset}_i-\text{onset}_i}\right)\right], & \text{onset}_i\le t\le\text{offset}_i\\ 0, & \text{otherwise}\end{cases}$$

where the excitation magnitude $e(t)$ depended on time (t) and amplitude (a_i), onset (onset_i), and offset (offset_i) of each mode (i). A first-order differential equation using time constants based on Winters and Stark (1988) was used to model the activation-deactivation dynamics (Raasch et al., 1997).

2.3. Energy storage and return prosthetic foot model

The prosthetic foot was modeled using 22 rigid segments, with the foot shape described by two spline curves (Fig. 2). The foot shape closely matched previously-manufactured SLS ESAR feet, which were based on a commonly prescribed commercial carbon fiber ESAR foot (Highlander, FS 3000, Freedom Innovations, LLC), and used in a human subject experiment with amputee participants (Fey et al., 2011; South et al., 2010).

At each rotational degree-of-freedom in the prosthetic foot model, a visco-elastic element applied a passive torque:

$$\tau_i=-k_i\theta_i-b\dot{\theta}_i$$

where each passive torque (τ_i) depended on element stiffness (k_i), angular displacement (θ_i) and angular velocity ($\dot{\theta}_i$). A damping value $b=5.73$ N m s was used for each element (Fey et al., 2011). Three different prosthetic stiffness distributions (Fig. 3) were used that matched the stiffness levels from the previously manufactured nominal, compliant (50% less stiff) and stiff (50% more stiff) SLS ESAR prosthetic feet (Fey et al., 2011).

2.4. Dynamic optimization and experimental tracking data

Dynamic optimization was used to identify the muscle excitation parameters of each muscle group and the initial generalized velocities. A simulated annealing algorithm (Goffe et al., 1994) solved the optimal tracking problem to generate simulations of amputee walking with nominal, compliant and stiff feet. Group average experimental data of amputee subjects walking with each of the three SLS prosthetic feet were used as tracking data, while the objective functions also minimized the sum of squared individual muscle stresses. Subjects included 12 unilateral, below-knee amputees that walked overground at 1.2 m/s, while kinematic motion, GRF and surface electromyography (EMG) data were measured (see Fey et al., 2011).

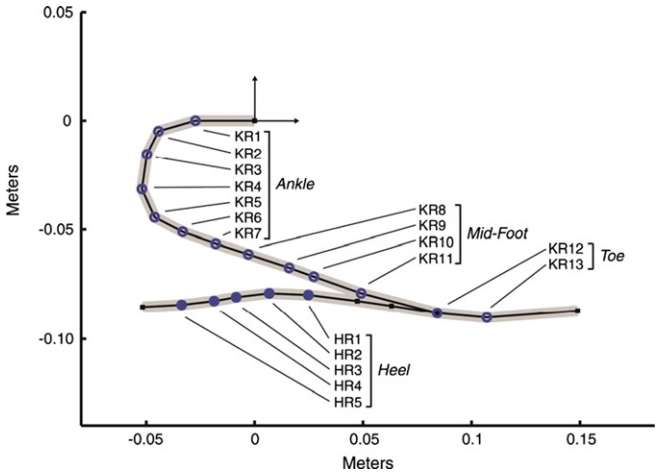

Fig. 2. The prosthetic foot model included 22 rigid segments connected in series by 13 keel (KR1-KR13, ○) and 5 heel (HR1-HR5, ●) revolute joints. Black squares indicate segment endpoints where rotational degrees-of-freedom are not present.

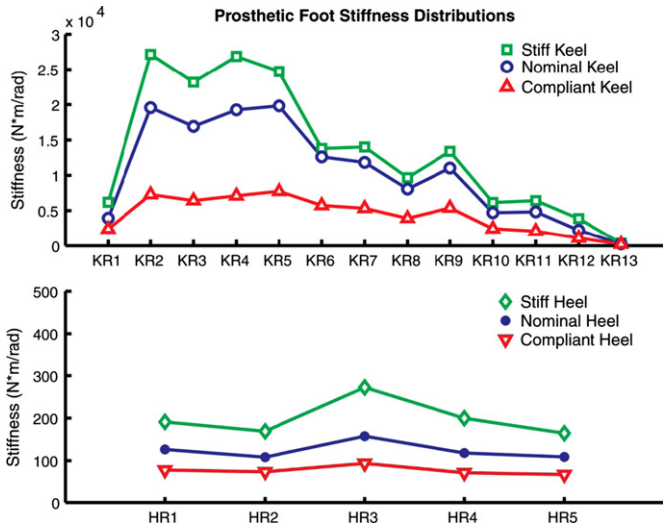

Fig. 3. Nominal, compliant and stiff prosthetic stiffness distributions of the keel (top) and heel (bottom) calculated from the three SLS ESAR feet analyzed by Fey et al. (2011). The SLS ESAR feet were previously manufactured from Rilsan™ D80 (Nylon 11, Arkema, Inc.) using a Vanguard HiQ Sinterstation (3D Systems, Inc.). Prosthetic foot segments were modeled as prismatic along their length and had material properties of laser-sintered Nylon 11.

2.5. Muscle and prosthetic foot function

To test our hypotheses, muscle and foot contributions to body support (vertical GRF), propulsion (anterior/posterior, A/P GRF) and residual leg swing (residual leg mechanical power) were compared using GRF decomposition (e.g., Neptune et al., 2001) and segment power (Fregly and Zajac, 1996) analyses. To gain further insight into the flow of mechanical power between body segments (i.e., the legs and trunk), contributions to horizontal and vertical power of the trunk were also calculated. Lastly, gravity contributions to body support and forward propulsion were computed since they have been shown to be substantial during walking (e.g., Lin et al., 2011) and may be influenced by stiffness. An increase or decrease in a quantity was considered to have occurred when the quantity changed by more than 10% relative to the other conditions.

3. Results

3.1. Experimental tracking data

The simulations emulated well the group average experimental data with average root-mean-square kinematic joint angle and GRF tracking deviations for all simulations of 10.0° and 0.09 GRF/BW, which were ~2 standard deviations of the experimental data (9.1° and 0.08 GRF/BW). For the simulation muscle groups in which experimental EMG data were collected, muscles were active during regions of the gait cycle when EMG activity were observed (Fig. 4).

3.2. Contributions to residual leg body support and propulsion

During the first half of stance, gravity and the prosthetic foot acted to brake the body (negative A/P GRF) and muscles produced propulsion (positive A/P GRF) (Fig. 5A). As stiffness decreased, these contributions from the prosthetic keel and muscles increased, while gravity contributions decreased. Also, the keel contributions to body support (positive vertical GRF) increased, while the heel and gravity contributions decreased (Fig. 5C).

During the second half of residual leg stance, keel contributions to propulsion decreased (Fig. 5B) and body support increased (Fig. 5D). In the compliant condition, gravity contributed to propulsion and muscles contributed to braking, which differed from the nominal and stiff conditions (Fig. 5B).

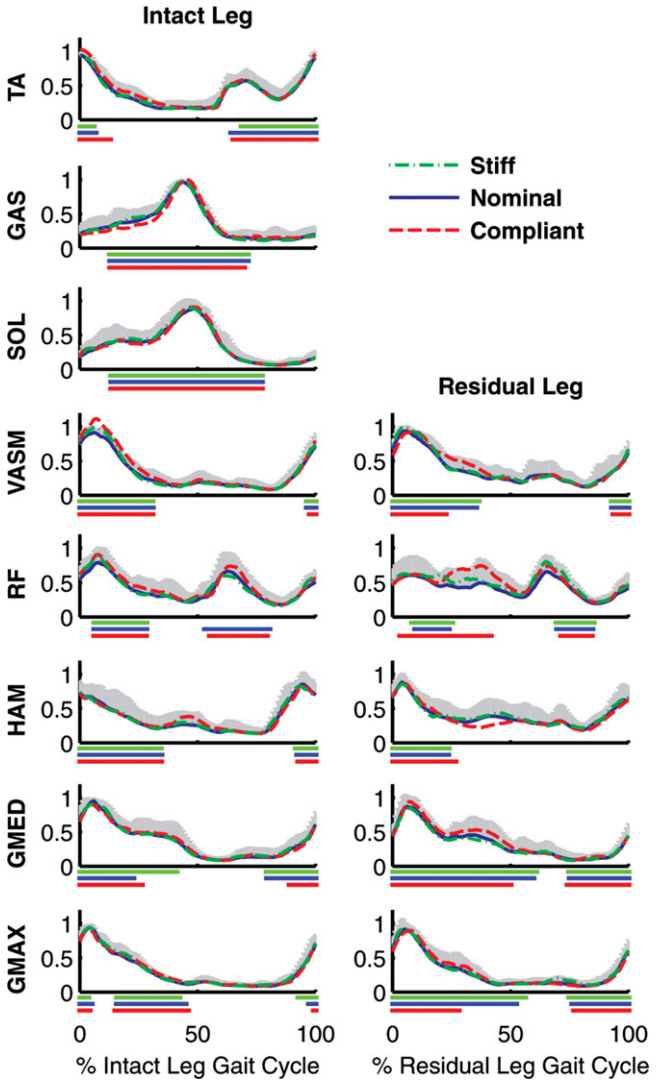

Fig. 4. Comparison of excitation timing with group average experimental EMG data of the amputee subjects (for only those muscles in which EMG data were collected). Group average experimental EMG data were normalized to the peak magnitude in the nominal condition prior to group averaging. Nominal EMG+1 SD are also plotted using vertical error bars. Excitation timing in the three simulations are plotted below each *x*-axis and correspond in color with the plotted EMG timing for each condition.

Muscle contributions to support and propulsion were also influenced by stiffness (Figs. 6 and 7). During the first half of residual leg stance, residual HAM, GMAX and GMED contributed to propulsion. The residual HAM contribution to propulsion had large increases as stiffness decreased, while GMAX and GMED contributions had smaller increases (Fig. 6A). Also, the residual RF contributed to braking during both the first and second halves of stance, which increased in the compliant condition (Figs. 6A and 6B).

Contrary to the first half of stance, the residual leg GMAX and GMED provided increased propulsion in the nominal and stiff conditions (as stiffness *increased*) during the second half of stance (Fig. 6B). Most residual leg muscle contributions to support were small during stance compared to the intact leg (compare Figs. 6C and 6D to Figs. 7C and 7D) because these functions were primarily performed by the prosthetic foot and gravity (Figs. 5C and 5D). However, the residual HAM provided substantial support during the first half of stance and decreased its contribution as stiffness decreased (Fig. 6C).

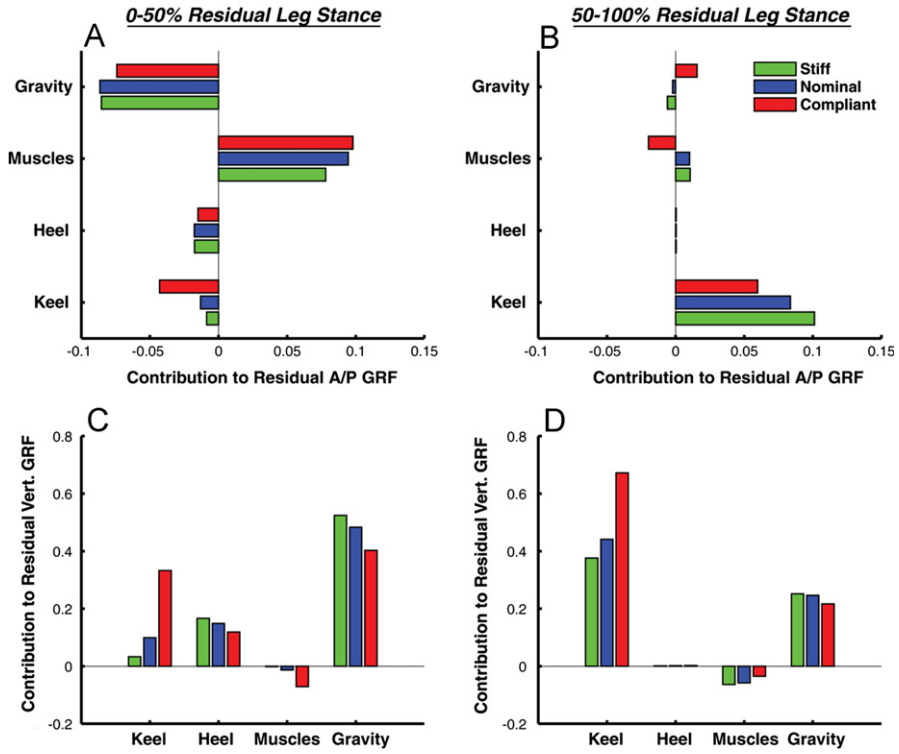

Fig. 5. Mean contributions of the prosthetic foot, residual and intact leg muscles, and gravity to the A/P and vertical GRF (GRF/body weight) of the residual leg. Data were averaged during the first (left column) and second (right column) halves of the residual leg stance phase.

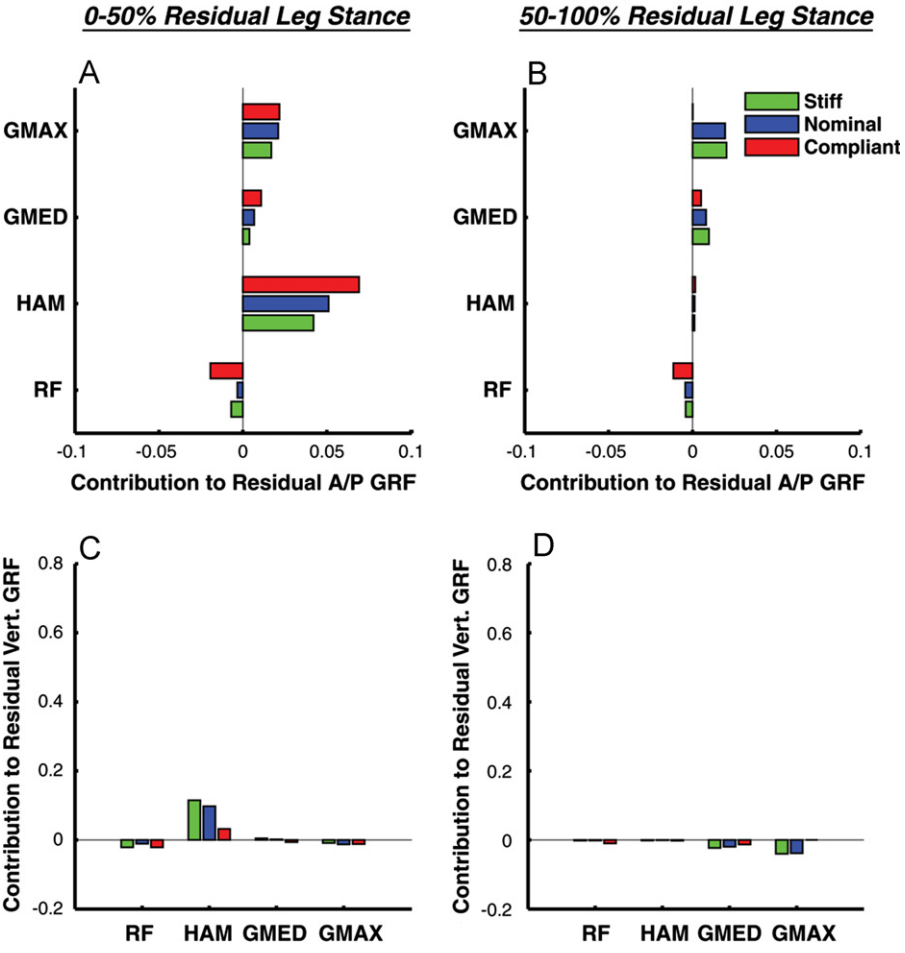

Fig. 6. Mean residual leg muscle contributions to the A/P and vertical GRF (GRF/body weight) of the residual leg. Data were averaged during the first (left column) and second (right column) halves of the residual leg stance phase.

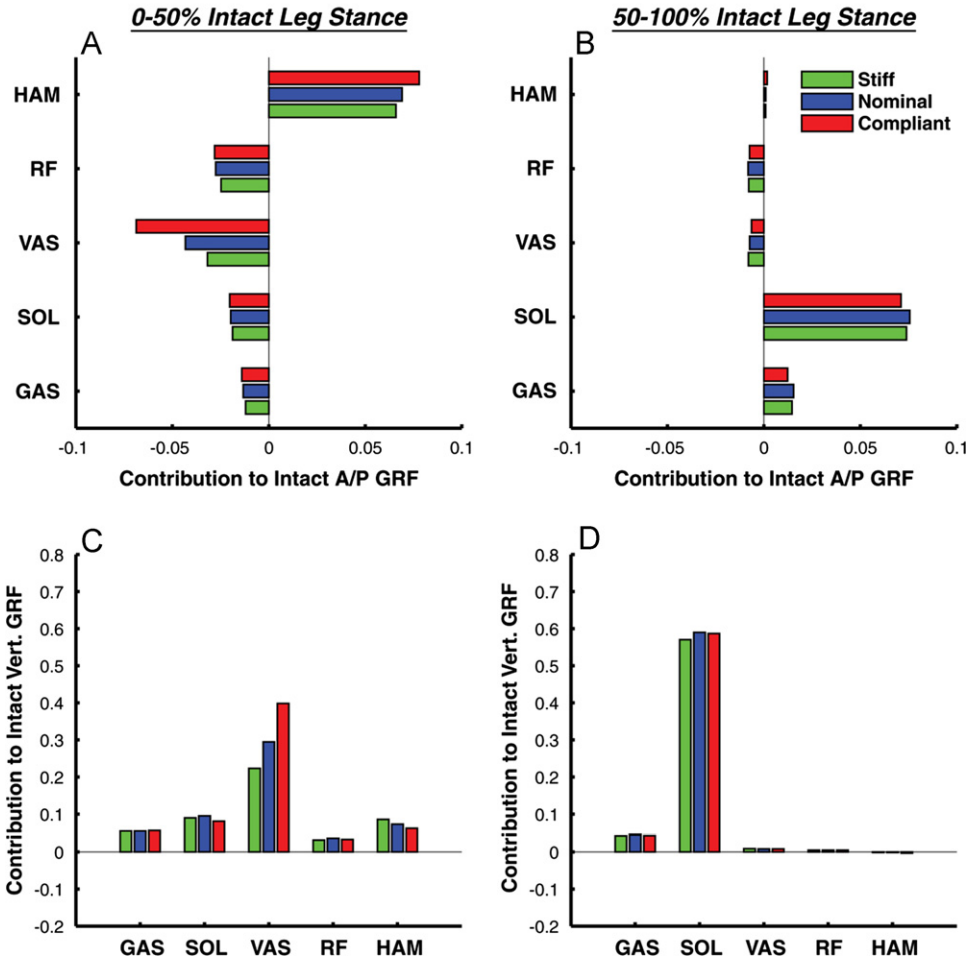

Fig. 7. Mean intact leg muscle contributions to the A/P and vertical GRF (GRF/body weight) of the intact leg. Data were averaged during the first (left column) and second (right column) halves of the intact leg stance phase. Contributions of VASL and VASM were summed (VAS) for these analyses.

3.3. Contributions to intact leg body support and propulsion

During the first half of intact leg stance, the intact leg RF, VAS, SOL and GAS contributed to body braking and HAM contributed to propulsion (Figs. 7A and 7C). These intact leg muscles provided body support, with the contributions from VAS being the largest. The largest intact-leg changes as stiffness decreased occurred in the VAS contributions to braking and support during this region (Figs. 7A and 7C). During the second half of intact leg stance, SOL and GAS were the primary contributors to body support and forward propulsion (Figs. 7B and 7D).

3.4. Contributions to residual leg swing

During the first half of residual leg stance, the residual leg muscles and prosthetic foot primarily absorbed leg power (Fig. 8A). As stiffness decreased, the keel absorbed more power while the residual leg RF absorbed more leg power in the compliant condition. Similarly, during the second half of residual leg stance, the residual leg RF absorbed more power (Fig. 8B). Unlike the trend observed during the first half of stance, the keel absorbed less power as stiffness decreased (Fig. 8B). During swing, the residual IL delivered power to the leg and the residual HAM absorbed power from the leg (Fig. 8C). The HAM contributions increased as stiffness decreased, while IL contributions had a small increase (i.e., 9%) between the compliant and stiff conditions.

3.5. Contributions to trunk power

During the first half of residual leg stance, the keel and heel acted to absorb horizontal power from the trunk (trunk braking), while the residual and intact leg muscles delivered horizontal power to the trunk (trunk propulsion) (Fig. 9A). As stiffness decreased, the keel absorbed less horizontal power. In addition, the keel provided greater vertical power to the trunk, while the residual leg HAM delivered less vertical power (Fig. 9D).

The largest changes in contributions to trunk power occurred during the second half of residual leg stance as stiffness decreased (Figs. 9B and 9E). The keel delivered the largest horizontal power to the trunk and absorbed the largest vertical power from the trunk, which decreased and increased, respectively, as stiffness decreased. The residual leg RF delivered increased horizontal power to the trunk (Fig. 9B) while the intact leg VAS absorbed increased horizontal power from the trunk and delivered increased vertical power to the trunk (Figs. 9B and 9E). Lastly, the intact leg VAS also delivered increased vertical power during swing of the residual leg (Fig. 9F).

3.5.1. Prosthetic foot energy storage and return

The total energy stored by the prosthetic feet during early and mid stance as well as the energy returned during late stance increased as stiffness decreased (Fig. 10).

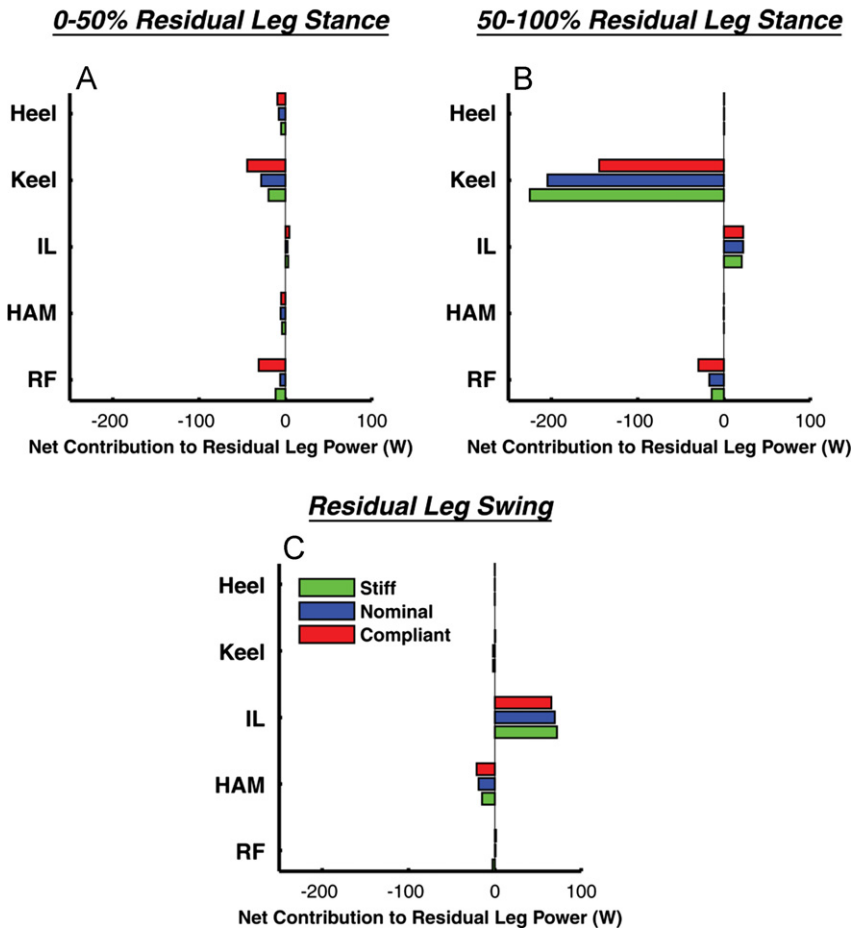

Fig. 8. Mean prosthetic foot and residual leg muscle contributions to total residual leg power. Data were averaged during the first (left column) and second (middle column) halves of residual leg stance and swing phases (right column).

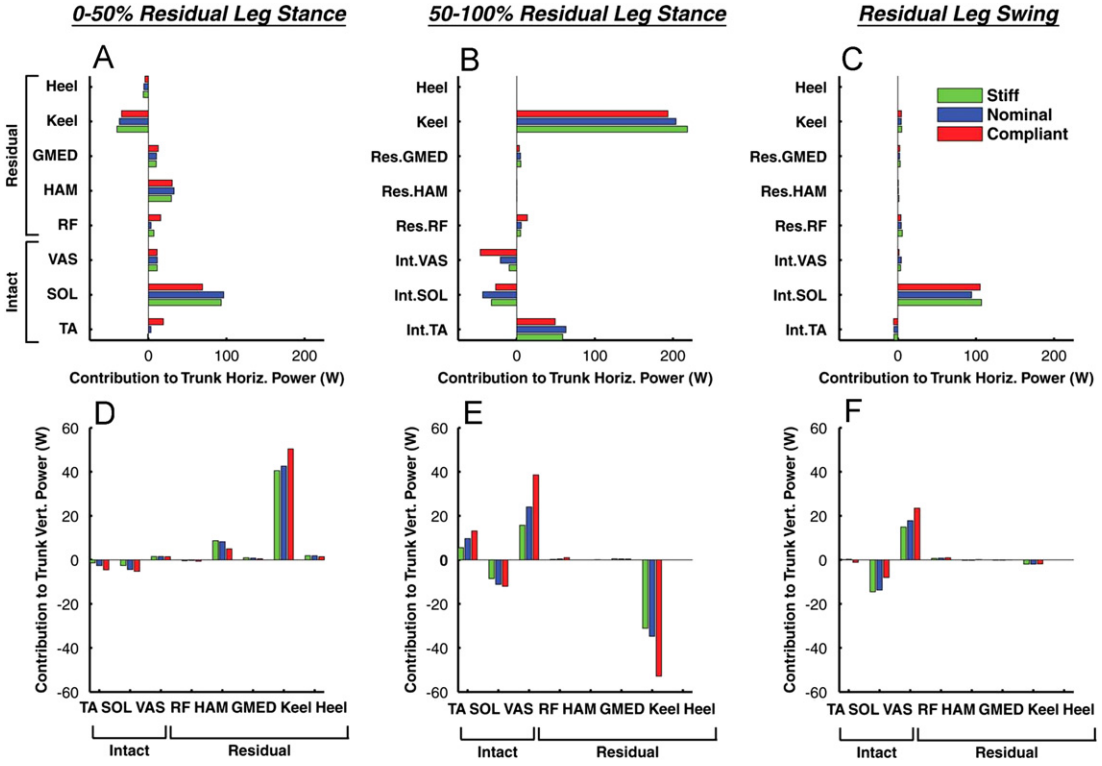

Fig. 9. Mean prosthetic foot and residual and intact leg muscle contributions to horizontal (top row) and vertical (bottom row) trunk power. Data were averaged during the first (left column) and second (middle column) halves of the residual leg stance and swing phases (right column).

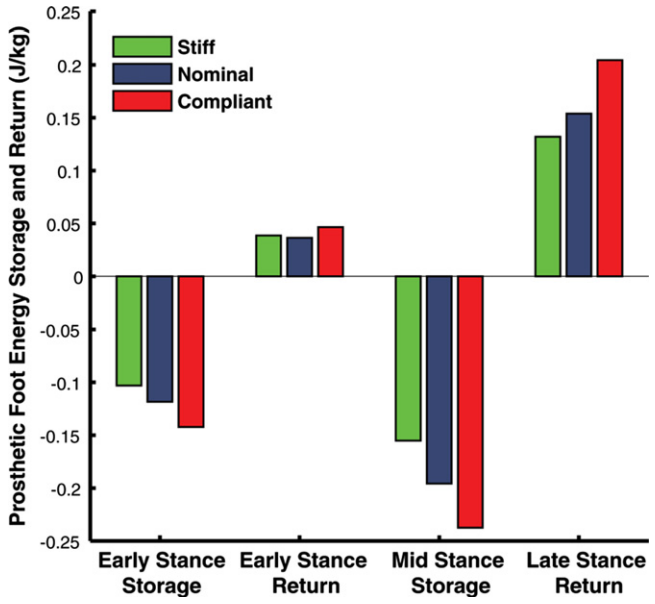

Fig. 10. Early stance energy storage, early stance energy return, mid stance energy storage, and late stance energy return of the prosthetic foot across stiffness conditions. The total energy was calculated by summing across rotational elements within each region of the foot and normalizing by body mass.

4. Discussion

Based on our previously-observed experimental findings (Fey et al., 2011), we hypothesized that as stiffness decreased, prosthetic foot contributions to propulsion and leg swing initiation would increase, and therefore muscle contributions to these subtasks would decrease. We also expected that foot contributions to body support would decrease as stiffness decreased, and therefore muscle contributions to support would increase. These hypotheses were only partially supported due to complex interactions between the prosthetic foot, muscles and body segments, and differences in the contributions of muscles and the prosthetic foot to walking subtasks throughout the gait cycle.

4.1. Influence of stiffness on body support and propulsion

During the first half of residual leg stance, as stiffness decreased the keel provided increased body support and braking (Figs. 5A and 5C), while the contributions to body support by the heel decreased. Thus, with the exception of the heel providing decreased body support, these results did not support our hypotheses. However, the increased keel contributions to braking was consistent with the experimental data showing an increased residual leg braking GRF in these subjects (Fey et al., 2011). The increased residual leg braking observed experimentally may be the result of increased keel contributions as stiffness decreased.

During the second half of residual leg stance, as stiffness decreased the keel provided increased body support and decreased forward propulsion (Figs. 5B and 5D), which did not support our hypotheses. However, a smaller residual leg vertical GRF was observed experimentally in the amputee subjects walking with the compliant foot during this region (Fey et al., 2011). Therefore, despite higher keel contributions to body support, the total body support by the residual leg was less, and may be limited during the second half of residual leg stance as stiffness decreases.

4.2. Influence of stiffness on residual leg swing

During the first half of stance, the keel absorbed increased power from the residual leg as stiffness decreased (Fig. 8A). Conversely, for swing initiation (i.e., power delivered to the residual leg prior to toe-off), the keel absorbed less power from the leg (Fig. 8B), and therefore contributed more to swing initiation. These results supported our hypotheses and were consistent with increased energy return in late stance found in this study (Fig. 10) and experimentally in these subjects (Fey et al., 2011). In addition, our results suggest that the reduced swing initiation as stiffness *increased* was compensated for by small increases in the energy delivered to the leg by residual leg IL and decreases in the absorption of leg energy by HAM during swing (Fig. 8C). The roles of these muscles were consistent with non-amputee walking (Neptune et al., 2004) and symmetric amputee walking (Zmitrewicz et al., 2007).

4.3. Influence of stiffness on residual leg compensations

As stiffness decreased, the primary compensatory mechanism for increased keel braking during the first half of residual leg stance was from the residual leg HAM, as it greatly increased its contribution to forward propulsion and decreased its contribution to body support (Figs. 6A and 6C). This compensation was possible since the keel provided increased body support. During the second half of residual leg stance, as stiffness decreased gravity contributed more to forward propulsion and less to body support, which compensated for a reduced contribution of the keel to propulsion, increased RF contribution to braking, and increased contribution of the keel to support (Figs. 5B, 5D and 6B). The contributions of RF to braking, and HAM and gravity to propulsion during stance are consistent with their roles during non-amputee walking (Lin et al., 2011; Liu et al., 2006; Neptune et al., 2004).

In these subjects, decreased residual leg biceps femoris longhead EMG (Fig. 4) was observed experimentally in the compliant condition during the second half of residual leg stance (Fey et al., 2011). Although not observed in these simulations, HAM can contribute to body propulsion throughout stance when it is active (Liu et al., 2006; Neptune et al., 2004). In addition, HAM also acts co-functionally with GMED and GMAX to provide propulsion during mid stance (Lin et al., 2011; Liu et al., 2006; Neptune et al., 2004). Decreased residual leg GMED and GMAX contributions to propulsion during the second half of stance were observed in the compliant condition (Fig. 6B). Thus, the decreased biceps femoris longhead EMG observed experimentally in the compliant condition may be related to the increased contributions of gravity to propulsion during the second half of stance and increased contributions of HAM to propulsion and/or increased GMED contributions to propulsion during the first half of stance (Fig. 6A).

An interesting finding was that throughout stance, the residual leg RF absorbed increased power from the leg (Figs. 8A and 8B) and contributed more to braking (Figs. 6A and 6B) as stiffness decreased. However, increased RF contributions to horizontal trunk power throughout stance were also observed (Figs. 9A and 9B). Thus, while the net effect of RF was to increase braking during stance by contributing negatively to the A/P GRF, through dynamic coupling of the leg and trunk body segments, RF transferred more power from the leg to the trunk to propel it forward. These increased residual leg RF compensations are consistent with increased EMG observed experimentally as stiffness decreased (Fig. 4). However, the increased residual leg RF EMG only approached significance due to a higher variability in these data across the subjects tested (Fey et al., 2011). The RF function to redistribute power from the leg to the trunk was consistent with its role in non-amputee walking (Neptune et al., 2004). Modulation of the residual leg RF function during amputee walking is an important mechanism to transfer increased

mechanical power from the leg to the trunk for propulsion as foot stiffness decreases (Fig. 8).

4.4. Influence of stiffness on intact leg compensations

As stiffness decreased, the increased intact leg VAS contributions to body support and braking partially supported our hypotheses (i.e., higher muscle contributions to support), suggesting additional intact leg body support is needed during the first half of intact leg stance. Previous work has identified the modulation of VAS contributions to these walking subtasks as an important compensatory mechanism when the demand for body weight support is modulated (McGowan et al., 2009). In addition, these compensations by VAS are consistent with the increased intact knee extensor moments, VAS EMG (Fig. 4), and intact leg braking GRF observed experimentally in these subjects as stiffness decreased (Fey et al., 2011). Thus, increased intact leg VAS contributions to body support appear to be an important mechanism for providing additional body support as stiffness decreases.

Another interesting finding was that during the first half of intact leg stance, as stiffness decreased the compensations of the intact leg VAS to provide increased body support (Fig. 7C) appears to be a primary mechanism compensating for increased vertical trunk power absorption by the keel during the second half of residual leg stance (Fig. 9E). These keel contributions were consistent with increased mid stance energy storage of the foot (Fig. 10) as well as the experimentally-observed increased dorsiflexion angle of the prosthetic foot as stiffness decreased in these subjects (Fey et al., 2011). During this region, the keel provided a vertical acceleration to the trunk as it moved downward, resulting in power absorption. Then, the intact VAS provided a vertical acceleration as the trunk moved upward, resulting in the delivery of vertical power. In addition, the increased positive contribution to vertical trunk power of the intact VAS during the second half of residual leg stance continued into the residual leg swing (Figs. 9E and 9F). As noted above, a consequence of the increased VAS contribution to support was an increase in its contribution to braking of the body (Fig. 6A) and trunk (Fig. 9B).

5. Conclusions

Overall, the identified functions of these ESAR prosthetic feet to provide body support and braking during the first half of stance and body support and forward propulsion during the second half of stance were consistent with the roles of the plantar flexor muscles (McGowan et al., 2009; Neptune et al., 2001). However, the function of the keel to primarily absorb power from the leg during the second half of stance is most consistent with the role of SOL in non-amputee walking, and not with the role of GAS, which provides swing initiation (Neptune et al., 2001).

In summary, altering ESAR prosthetic foot stiffness can significantly influence foot and residual and intact leg muscle function through out the entire gait cycle. Thus, given an amputee's functional deficits, the prescription of appropriate foot stiffness is important and may substantially influence their gait performance. This study identified important mechanisms that help modulate the performance of essential walking subtasks as foot stiffness is altered. Combining complex modeling of ESAR stiffness and forward dynamics simulations of walking enabled us to identify the dynamic interactions between the prosthetic foot and musculoskeletal system. This framework may prove useful in future studies that fine-tune foot design characteristics or evaluate foot prototypes prior to manufacture.

Conflict of interest statement

The authors have no conflict of interest to declare.

Acknowledgments

Funding for this study was provided by the National Science Foundation, Grant 0346514 and Department of Veterans Affairs, Grant 1 I01 RX000311.

References

Anderson, F.C., Pandy, M.G., 1999. A dynamic optimization solution for vertical jumping in three dimensions. Computer Methods in Biomechanics and Biomedical Engineering 2 (3), 201–231.
Anderson, F.C., Pandy, M.G., 2003. Individual muscle contributions to support in normal walking. Gait & Posture 17 (2), 159–169.
Burke, M.J., Roman, V., Wright, V., 1978. Bone and joint changes in lower limb amputees. Annals of the Rheumatic Diseases 37 (3), 252–254.
Davy, D.T., Audu, M.L., 1987. A dynamic optimization technique for predicting muscle forces in the swing phase of gait. Journal of Biomechanics 20 (2), 187–201.
Delp, S.L., Loan, J.P., Hoy, M.G., Zajac, F.E., Topp, E.L., Rosen, J.M., 1990. An interactive graphics-based model of the lower extremity to study orthopaedic surgical procedures. IEEE Transactions on Biomedical Engineering 37 (8), 757–767.
Fey, N.P., Klute, G.K., Neptune, R.R., 2011. The influence of energy storage and return foot stiffness on walking mechanics and muscle activity in below-knee amputees. Clinical Biomechanics (Bristol, Avon) 26 (10), 1025–1032.
Fregly, B.J., Zajac, F.E., 1996. A state-space analysis of mechanical energy generation, absorption, and transfer during pedaling. Journal of Biomechanics 29 (1), 81–90.
Goffe, W.L., Ferrier, G.D., Rogers, J., 1994. Global optimization of statistical functions with simulated annealing. Journal of Econometrics 60 (1–2), 65–99.
Hall, A.L., Peterson, C.L., Kautz, S.A., Neptune, R.R., 2011. Relationships between muscle contributions to walking subtasks and functional walking status in persons with post-stroke hemiparesis. Clinical Biomechanics (Bristol, Avon) 26 (5), 509–515.
Lin, Y.-C., Kim, H.J., Pandy, M.G., 2011. A computationally efficient method for assessing muscle function during human locomotion. International Journal for Numerical Methods in Biomedical Engineering 27 (3), 436.
Liu, M.Q., Anderson, F.C., Pandy, M.G., Delp, S.L., 2006. Muscles that support the body also modulate forward progression during walking. Journal of Biomechanics 39 (14), 2623–2630.
Mattes, S.J., Martin, P.E., Royer, T.D., 2000. Walking symmetry and energy cost in persons with unilateral transtibial amputations: matching prosthetic and intact limb inertial properties. Archives of Physical Medicine and Rehabilitation 81 (5), 561–568.
McGowan, C.P., Kram, R., Neptune, R.R., 2009. Modulation of leg muscle function in response to altered demand for body support and forward propulsion during walking. Journal of Biomechanics 42 (7), 850–856.
Neptune, R.R., Wright, I.C., Van Den Bogert, A.J., 2000. A method for numerical simulation of single limb ground contact events: application to heel-toe running. Computer Methods in Biomechanics and Biomedical Engineering 3 (4), 321–334.
Neptune, R.R., Kautz, S.A., Zajac, F.E., 2001. Contributions of the individual ankle plantar flexors to support, forward progression and swing initiation during walking. Journal of Biomechanics 34 (11), 1387–1398.
Neptune, R.R., Zajac, F.E., Kautz, S.A., 2004. Muscle force redistributes segmental power for body progression during walking. Gait & Posture 19 (2), 194–205.
Raasch, C.C., Zajac, F.E., Ma, B., Levine, W.S., 1997. Muscle coordination of maximum-speed pedaling. Journal of Biomechanics 30 (6), 595–602.
Sanderson, D.J., Martin, P.E., 1997. Lower extremity kinematic and kinetic adaptations in unilateral below-knee amputees during walking. Gait & Posture 6, 126–136.
South, B.J., Fey, N.P., Bosker, G., Neptune, R.R., 2010. Manufacture of energy storage and return prosthetic feet using selective laser sintering. Journal of Biomechanical Engineering 132 (1), 015001.
Winter, D.A., Sienko, S.E., 1988. Biomechanics of below-knee amputee gait. Journal of Biomechanics 21 (5), 361–367.
Winters, J.M., Stark, L., 1988. Estimated mechanical properties of synergistic muscles involved in movements of a variety of human joints. Journal of Biomechanics 21 (12), 1027–1041.
Zajac, F.E., 1989. Muscle and tendon: properties, models, scaling, and application to biomechanics and motor control. Critical Reviews in Biomedical Engineering 17 (4), 359–411.
Zmitrewicz, R.J., Neptune, R.R., Sasaki, K., 2007. Mechanical energetic contributions from individual muscles and elastic prosthetic feet during symmetric unilateral transtibial amputee walking: a theoretical study. Journal of Biomechanics 40 (8), 1824–1831.